Theoretical Chemistry Accounts (2020) 139:139
https://doi.org/10.1007/s00214-020-02655-3

REGULAR ARTICLE

A theoretical study on water-assisted excited state double proton transfer process in substituted 2,7-diazaindole-H_2O complex

Hua Fang[1]

Received: 29 April 2020 / Accepted: 23 July 2020 / Published online: 3 August 2020

Abstract
The substituted effect on the first excited-state proton transfer (ESPT) process in 2,7-diazaindole-H_2O (2,7-DAI-H_2O) complex in water was studied in detail at the TD-M06-2X/6–311 + G(d, p) level. The frontier molecular orbital, geometries, reaction mechanism and energies of ESPT process with different substituent have been analyzed. ESPT process in the title complex occurred concertedly but highly asynchronously no matter of the electronic nature of substituent. The absorption and fluorescence peaks, H-bond distances, asynchronicity of ESPT and barrier height were affected by the substituent. The Hammett's substituent constant had linear correlation with the difference between the sum of N_1−O_{11} and O_{11}−N_7 distances in the reactant and that in the TS and Mulliken charge of H_3O^+.

Keywords Excited-state · Proton transfer · Substituent effect · Concerted · Asynchronous

1 Introduction

Hydrogen bond (H-bond) is one of the most fundamental weak interactions in nature and the basis of maintaining life-cycle [1–3]. It plays important parts in some microstructures of molecules and supramolecules, such as the complex of solute and solvent, polymers, proteins and DNA.[4–6]. Recently, hydrogen bonding (H-bonding) dynamics has attracted a lot of attention since Han et al. proposed a new mechanism that H-bond is enhanced in the electronic excited state [7–11]. H-bonding interaction can reasonably interpret many various mechanisms in the excited state. Proton transfer (PT) is one of the most significant chemical reactions along H-bond and broadly exists in biological and chemical field. Especially, excited-state proton transfer (ESPT) reaction has received great attention due to its unique photochemical and photophysical properties.

Compounds with ESPT behavior have a proton donor (−OH or –NH group) and a proton acceptor (−C = O or –N = N group) which are far away from each other and can transfer the proton with the assistance of the protic solvent serving as a bridge via forming a H-bonded network between the proton donor and proton acceptor [12]. When the proton donor and proton acceptor are close to each other, excited-state proton transfer can occur along the intramolecular H-bond, and it is called excited-state intramolecular proton transfer (ESIPT) [13, 14]. ESPT and ESIPT reactions takes place on ultrafast time scale within 100 fs. Recently, ESPT reactions have been widely studied on the detailed mechanism and some parameters relate to control ESPT process [15–24]. The dynamics of ESPT process is related to the strength of H-bond. Among all kinds of ESPT molecules, 7-azaindole (7AI) is an important model molecule because of its similar structures of DNA base pair and its application in probing protein structure [25–27]. 7AI contains both proton donor (N–H) and acceptor (=N−) and can form a cyclic H-bonding structure between proton donor and proton acceptor via dimerization [28–42] or solvent mediated [26, 27, 43–45] which may provide an effective path to transport a proton from N–H to =N−. 7AI molecule has dual emission behavior in alcohol, while in pure water there is only a single fluorescence band at 385 nm.

Several research groups have investigated the fluorescence emission of 7AI in water and draw different conclusions on its source and mechanism. This emission band was originally designated as a strong red-shifted normal emission [46], and it was suggested to be caused by the formation of exciplex (7AI/water) [47]. Negrerie et al. [27] reassigned

✉ Hua Fang
susanfang20@gmail.com

[1] Department of Chemistry and Material Science, College of Science, Nanjing Forestry University, Nanjing 210037, People's Republic of China

the 385 nm band to the emission of tautomer generated by excited state double proton transfer (ESDPT). Chou et al. [48] observed a weak emission peak at ~ 500 nm which was originated from ESDPT of 7AI-water H-bonded complex. Chapman et al. [49] reported that the spectral properties of 7AI in water and alcohol were different. The difference in the spectrum was owing to the different rate. Petrich et al. [50] explained the spectrum of 7AI in water and proposed that only a small amount (20%) of 7AI could occur ESPT on a time scale of 1 ns. They also pointed out that the tautomer emission of 7AI in water could be ignored because of the rapid protonation of tautomer species, which led to the tautomer cation (~ 440 nm) emission hidden in the main normal (385 nm) emission.

7-Azatryptophan has long been used as a probe to study the structure and kinetics of proteins [26]. 7-azatryptophan has a longer absorption spectral onset and a polar sensitive emission peak wavelength. However, the photophysical properties in water of 1-azatryptophan are similar to that of 7AI, namely, no tautomer emission has been observed [51–54]. Therefore, 7-azatryptophan cannot be used to detect any water-related photophysical phenomena in proteins. In order to overcome the limitations of 7AI and 7-azatryptophan, Chou et al. [55] developed a new probe, 2,7-diazaindole (2,7-DAI) (see Fig. 1), which could sense a protein in water environment. In 2,7-DAI, N_2 atom acts as an efficient electron-withdrawing group [56], which can improve the acidity of N_1−H group without affecting the parent structure. In pure water, 2,7-DAI showed distinct triple fluorescence bands in the excited state, that was an obvious shoulder at ~ 330 nm, a peak wavelength at ~ 370 nm and a large red-shifted emission band at ~ 500 nm, which was corresponding to N_1−H, N_2−H and N_7−H isomers, respectively. The triple emission has been rationalized by ground state and excited-state proton transfer processes. Similar to 7AI, 2,7-DAI can occur excited-state proton transfer along the intermolecular H-bonded chain with the assistance of polar solvent (H_2O, NH_3, CH_3OH, etc.). Taking 2,7-DAI as the core part, a new tryptophan analogue, 2,7-diazatryptophan, which displayed apparent water-assisted proton transfer tautomerization and had an advantage of water molecule sensing in proteins was developed. Hence, detailed study on 2,7-DAI is very necessary. Li et al. [57] studied the water-catalyzed ESPT process in the 2,7-DAI-$(H_2O)_2$ complex theoretically. Their results showed that the H-bonds were enhanced in the excited state which could accelerate the ESPT process. The transfer of H_1 from N_1 to O_1 in 2,7-DAI-$(H_2O)_2$ complex was more easier due to the lower potential barrier energy (6.99 kcal/mol). Since no stable intermediate has been obtained during the ultrafast ESPT process, they could not conclude that excited-state proton transfer occurred concertedly or stepwisely. Our group has investigated the ESPT processes occurring from N_1−H isomer to N_2−H (path 1) or N_7−H (path 2) isomers of 2,7-DAI-H_2O complex theoretically [58]. The two ESPT reactions in 2,7-DAI-H_2O complex both took place in a concertedly but asynchronously protolysis mechanism. The excited state double proton transfer tended to occur between N_1−H and N_7−H isomers since the ESPT barrier height of path 2 is 13.7 kcal/mol lower than that of path 1. We also considered the substituted effect on the ESPT process in 2,7-DAI-H_2O complex. The substituted halogen atom did not influence the ESPT mechanism, but changed the structural parameter, reduced the barrier height of 2,7-DAI-H_2O, and enlarged the asynchronicity of ESPT process.

Recently, the substituent effect on proton transfer process has aroused great interest of many researchers [59–63]. A large number studies showed that ESPT dynamics was closely correlated with the substituent properties and substituted positions. The introduction of different functional groups to modify the molecular structures has been proved to be an effective strategy to design new ESPT molecules with specific functions. Hence, in order to illustrate the

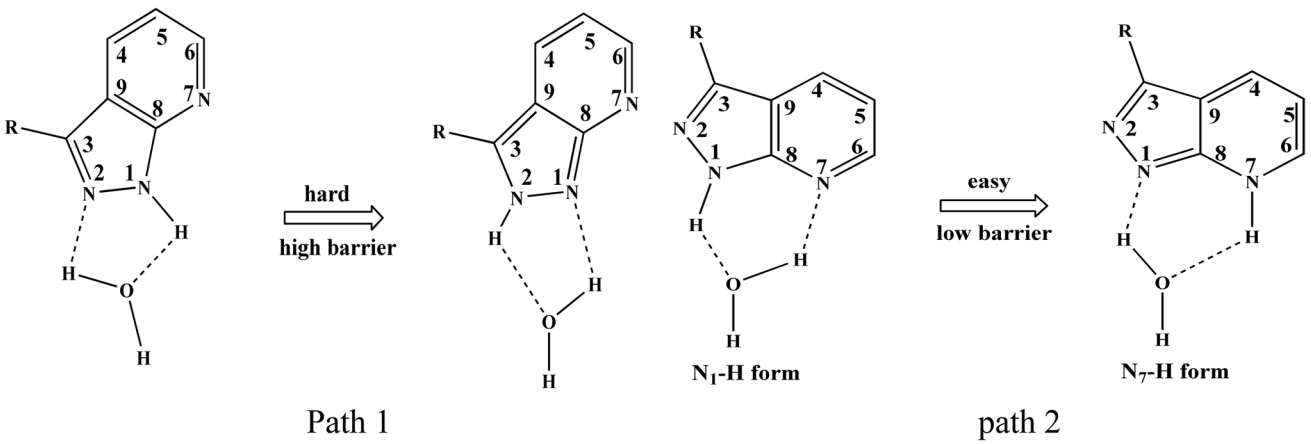

Fig. 1 The proposed water-catalyzed excited-state proton transfer (ESPT) mechanism for 3-*R*-2,7-DAI-H_2O (*R*: H, CH_3, C_2H_5, NH_2, CF_3, CN)

relationship between ESPT dynamics and substituted group, we performed a deeper insight into the ESPT process in the 2,7-DAI-H_2O derivatives. In 2,7-DAI-H_2O, electron-donating or electron-withdrawing group *R* (CH_3, C_2H_5, NH_2, CF_3, CN) is substituted for the H atom at C_3 position since this position is the closest position to proton donor (N–H) of 2,7-DAI-H_2O. Our theoretical calculations have been proved that the closer the substituent is to the proton donor, the lower the barrier height of ESPT, and more favorable for proton transfer [64]. Hence, 2,7-DAI-H_2O derivatives is denoted as 3-*R*-2,7-DAI-H_2O. The purpose of this study is to investigate the electron effect of the substituent on the ESPT thermodynamics and kinetics. Our work will provide some valuable information for designing new ESPT molecule.

2 Computational details

All the quantum chemical calculations were accomplished by using Gaussian 09 program [65]. The ESPT process in the 2,7-DAI-H_2O complex may take place in two pathways and produce two different tautomers (see Fig. 1). Since the ESPT process between N_1−H and N_2−H isomers is difficult to occur due to its high barrier height based on our previous studies [58], we only consider the substituent effect on the ESPT reaction between N_1−H and N_7−H isomers. The first excited state (S_1) optimized structures of reactant, product and transition state (TS) in the 3-*R*-2,7-DAI-H_2O (*R*: CH_3, C_2H_5, NH_2, CF_3, CN) complex and vibrational frequencies calculations were performed with TD-M06-2X [66] method and 6–311 + G(d, p) basis set. There is no imaginary frequency for the reactant and product, and only one imaginary frequency for TS. Solvent effect is considered via the integral equation formalism polarizable continuum model (IEFPCM) [67–69]. Water with a dielectric constant of 78.3 was used as solvent. The ground state (S_0) optimized structures of 3-*R*-2,7-DAI-H_2O were obtained at the M06-2X/6–311 + G(d,p)/IEFPCM level. Based on the S_0 and S_1 optimized structures, the absorption and fluorescence spectral data were calculated at the TD-M06-2X/6–311 + G(d,p)/IEFPCM level.

3 Results and discussion

3.1 Frontier molecular orbitals

At first, we investigated the nature of electron distribution of 3-*R*-2,7-DAI-H_2O (*R*: CH_3, C_2H_5, NH_2, CF_3, CN) complex in the first excited state before analyzing the ESPT dynamics since the nature of ESPT process in the heteroaromatic molecules and their H-bonded complexes was influenced by the relative energy of the $S_{\pi\pi^*}$ and $S_{\pi\sigma^*}$ states. Excited state hydrogen atom transfer (ESHAT) occurs in the $\pi\sigma^*$ state, while ESPT occurs in the $\pi\pi^*$ state [70–73]. The highest occupied molecular orbital (HOMO) and the lowest unoccupied molecular orbital (LUMO) of 3-*R*-2,7-DAI-H_2O (*R*: CH_3, C_2H_5, NH_2, CF_3, CN) complex are displayed in Fig. 2 since the first excited state of 3-*R*-2,7-DAI-H_2O was mainly related to the transition between HOMO and LUMO (see Table 1). HOMO and LUMO of 3-*R*-2,7-DAI-H_2O show π and π^* character, respectively, which confirms that the S_1 state has obvious $\pi\pi^*$ feature. The whole electron density of HOMO and LUMO is distributed on 3-*R*-2,7-DAI-H_2O, and no electron density is distributed on water and the H-bonded chain. Namely, water and the H-bonded chain are still in S_0 state during PT process. The π and π^* feature of HOMO and LUMO in 3-*R*-2,7-DAI-H_2O were not affected by the substituted group R.

We also calculated the maximum absorption and dual fluorescence emission peaks of 3-*R*-2,7-DAI-H_2O (*R*: CH_3, C_2H_5, NH_2, CF_3, CN) based on the optimized structures in the S_0 and S_1 states, respectively. As shown in Table 1, the calculated absorption and fluorescence emission peaks of 2,7-DAI-H_2O are consistent with the experimental values [55], which proves that our theoretical results of 3-*R*-2,7-DAI-H_2O (*R*: CH_3, C_2H_5, NH_2, CF_3, CN) are reliable. It is obvious that the substituent R influences the absorption and the fluorescence peaks of 3-*R*-2,7-DAI-H_2O. For 3-*R*-2,7-DAI-H_2O (*R*: CH_3, C_2H_5, NH_2) complex, the absorption peak and the fluorescence peaks of N_1−H and N_7−H forms locate at 269−283 nm, 323−354 nm and 465–542 nm, respectively. When the electron-withdrawing group (CF_3, CN) replaced the H atom at C_3 position in the 2,7-DAI-H_2O complex, the corresponding absorption peak and fluorescence peaks of N_1−H and N_7−H forms are at 255–60, 296–298 and 386–388 nm, respectively. It is obvious that the Stokes shift of 3-*R*-2,7-DAI-H_2O (*R*: CH_3, C_2H_5, NH_2, CF_3, CN) complex changes with the substituent R.

3.2 ESPT mechanism

The structural parameters of reactant, product and TS in the 3-*R*-2,7-DAI-H_2O (*R*: CH_3, C_2H_5, NH_2, CF_3, CN) complex are listed in Table 2. The geometries of TS are shown in Fig. 3. For the 3-*R*-2,7-DAI-H_2O (*R*: CH_3, C_2H_5, NH_2, CF_3, CN) complex, there is only one TS but no intermediate obtained during the ESPT process. As shown in Table 2, the N_1−H_{10}, H_{10}−O_{11}, O_{11}−H_{12} and H_{12}−N_7 distances of 3-*R*-2,7-DAI-H_2O (*R*: CH_3, C_2H_5, NH_2, CF_3, CN) are in the range of 1.309–1.357 Å, 1.154–1.195 Å, 1.029–1.103 Å and 1.452 ~ 1.670 Å, respectively. The N_1−H_{10} distance of 3-*R*-2,7-DAI-H_2O is on average 0.157 Å longer than the corresponding H_{10}−O_{11} distance, and the O_{11}−H_{12} distance is on average 0.512 Å shorter than the corresponding H_{12}−N_7 distance. This result indicates that the proton H_{10} transfers

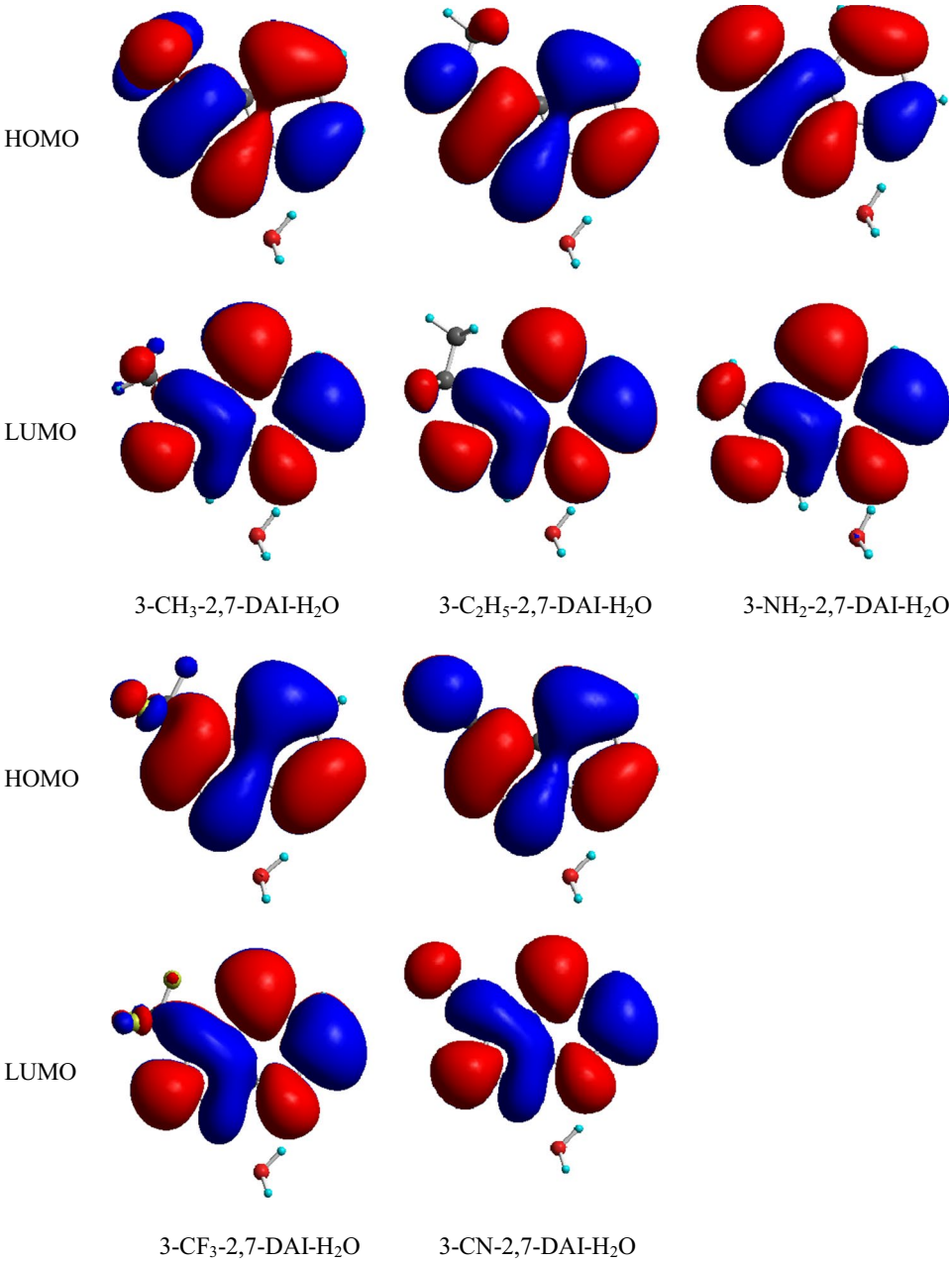

Fig. 2 The frontier molecular orbitals of 3-*R*-2,7-DAI-H_2O (*R*: CH_3, C_2H_5, NH_2, CF_3, CN) complex in the first excited-state (S_1) in water

Table 1 Maximum absorption and fluorescence emission wavelengths (nm), oscillator strengths (in parenthesis) and the corresponding orbital transition contributions of electronic excitation of $S_0 \rightarrow S_1$ for 3-*R*-2,7-DAI-H_2O (*R*: H, CH_3, C_2H_5, NH_2, CF_3, CN) complex in S_1 state

System	λ_{abs}	λ_{em} [a]	λ_{em} [b]	Orbital contributions
2,7-DAI-H_2O[c]	295	335	495	
2,7-DAI-H_2O[d]	261(0.21)	305(0.19)	419	HOMO → LUMO 97.4%
3-CH_3-2,7-DAI-H_2O	269(0.20)	323(0.15)	465	HOMO → LUMO 97.7%
3-C_2H_5-2,7-DAI-H_2O	269(0.20)	330(0.15)	470	HOMO → LUMO 98.0%
3-NH_2-2,7-DAI-H_2O	299(0.15)	413(0.08)	671	HOMO → LUMO 98.8%
3-CF_3-2,7-DAI-H_2O	255(0.27)	296(0.25)	386	HOMO → LUMO 97.7%
3-CN-2,7-DAI-H_2O	260(0.38)	298(0.28)	388	HOMO → LUMO 96.9%

[a]Fluorescence emission peak of N_1−H form

[b]Fluorescence emission peak of N_7−H form

[c]Experimental values from Ref. [55]

[d] Theoretical values from Ref. [58]

Table 2 Geometric parameters (Å) of reactant, product, and transition state (TS) for excited-state proton transfer in the 3-*R*-2,7-DAI-H_2O (*R*: H, CH_3, C_2H_5, NH_2, CF_3, CN) complex in the S_1 state

	System	$r(N_1-H_{10})$	$r(H_{10}-O_{11})$	$r(O_{11}-H_{12})$	$r(H_{12}-N_7)$
Reactant	2,7-DAI-H_2O[a]	1.028	1.940	0.977	1.951
	3-CH_3-2,7-DAI-H_2O	1.028	1.948	0.978	1.923
	3-C_2H_5-2,7-DAI-H_2O	1.027	1.949	0.978	1.923
	3-NH_2-2,7-DAI-H_2O	1.024	1.995	0.982	1.875
	3-CF_3-2,7-DAI-H_2O	1.031	1.896	0.973	2.026
	3-CN-2,7-DAI-H_2O	1.032	1.887	0.973	2.036
TS	2,7-DAI-H_2O[a]	1.331	1.174	1.055	1.572
	3-CH_3-2,7-DAI-H_2O	1.323	1.182	1.065	1.541
	3-C_2H_5-2,7-DAI-H_2O	1.324	1.181	1.069	1.530
	3-NH_2-2,7-DAI-H_2O	1.309	1.195	1.103	1.452
	3-CF_3-2,7-DAI-H_2O	1.347	1.161	1.031	1.662
	3-CN-2,7-DAI-H_2O	1.357	1.154	1.029	1.670
Product	2,7-DAI-H_2O[a]	2.090	0.968	1.997	1.018
	3-CH_3-2,7-DAI-H_2O	2.061	0.969	2.016	1.017
	3-C_2H_5-2,7-DAI-H_2O	2.048	0.970	2.019	1.017
	3-NH_2-2,7-DAI-H_2O	1.991	0.972	2.053	1.016
	3-CF_3-2,7-DAI-H_2O	2.172	0.967	1.962	1.020
	3-CN-2,7-DAI-H_2O	2.181	0.967	1.954	1.020

[a]Data from Ref. [58]

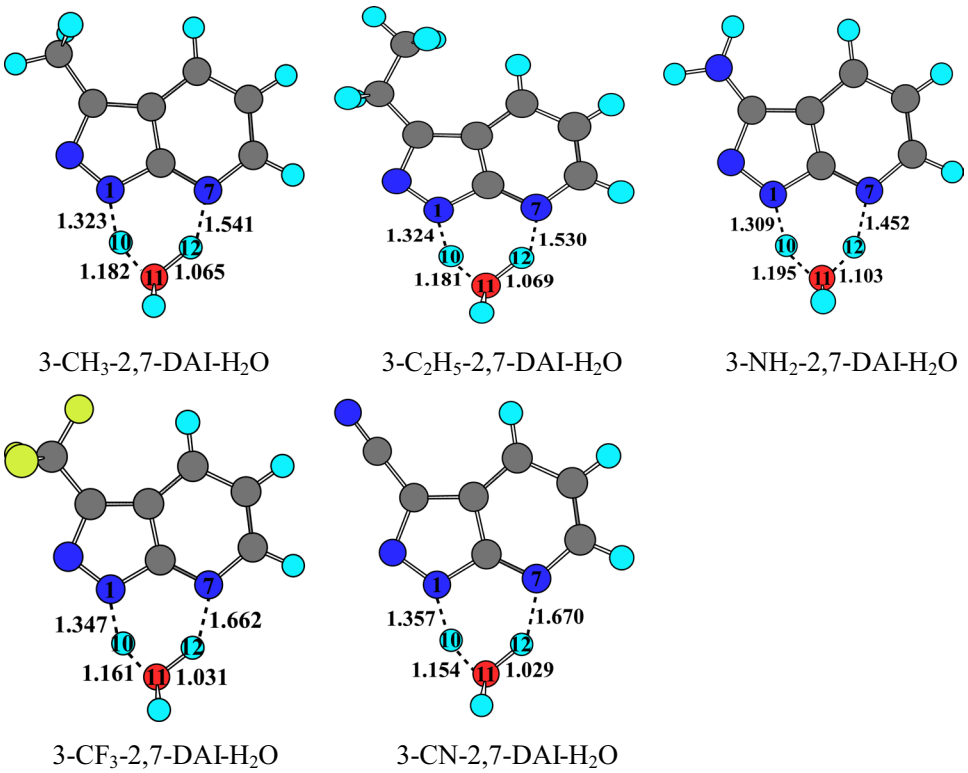

Fig. 3 TS structures of ESDPT in the 3-*R*-2,7-DAI-H_2O (*R*: CH_3, C_2H_5, NH_2, CF_3, CN) complex in water. Bond distances are in Å

first and moves more than halfway from N_1 to O_{11}, the proton H_{12} transports a little from O_{11} to N_7 subsequently, and a H_3O^+-like moiety is generated at O_{11}. ESPT process in the 3-*R*-2,7-DAI-H_2O complex takes place via an asynchronous but concerted protolysis [74] pattern. The Mulliken charges of the H_3O^+-portion of TS in the 3-*R*-2,7-DAI-H_2O complex are in the range of 0.752–0.859 a.u. (see Table 3), which are because asynchronous transfer of H_{10} and H_{12} makes both protons are close O_{11}, and hence, a H_3O^+-portion of TS generates. It is evident that the Mulliken charges in Table 3

confirm the mechanism of ESPT in the 3-*R*-2,7-DAI-H_2O complex.

We also depicted a correlation plot between proton transfer coordinate and the H-bond distance during proton transfer process visually. The H-bond coordinates $q_1 = 1/2 (r_{XH} - r_{YH})$ and $q_2 = r_{XH} + r_{YH}$ can be used to describe the H-bond distance (r_{XH} and r_{YH}) in the X–H…Y complex [76–78]. In the X–H…Y complex, based on the assumption of total bond order conservation, the r_{XH} and r_{YH} distances conform to the Pauling equations and are correlated with each other [79].

$$n_{XH} = \exp\{-(r_{XH} - r^0_{XH})/b_{XH} \quad (1)$$

$$n_{YH} = \exp\{-(r_{YH} - r^0_{YH})/b_{YH} \quad (2)$$

where $r_{XH}{}^0$ and $r_{YH}{}^0$ are bond distances in free XH and YH, and b_{XH} and b_{YH} are parameters describing bond valences decay [80]. For a linear H-bond, the distance from H to the H-bonding center is expressed by q_1, and the distance from X to Y is expressed by q_2. Bond distance correlates with bond energy and bond order. The characteristics of TS (e.g., earliness or lateness, bond order, synchronicity) can be investigated by this correlation [81, 82]. When H migrates from X to Y in the X–H…Y complex, q_1 will change from negative to positive, and q_2 will experience a minimum and locate at $q_1 = 0$. The negative or positive q_1 value of TS means an early or a late TS, respectively. The small or big q_2 value of TS means a tight or a loose TS. When more than one proton moves in the synchronous or asynchronous pattern, the multiple q_1 values of TS would be very similar or different, respectively.

The correlation between N_1–H_{10} and H_{10}–O_{11} distances (H_{10} transfer), and O_{11}–H_{12} and H_{12}–N_7 distances (H_{12} transfer) for the 3-*R*-2,7-DAI-H_2O (*R*: CH_3, C_2H_5, NH_2, CF_3, CN) complex are displayed in Fig. 4. The stationary points (reactant, TS and product) of 3-*R*-2,7-DAI-H_2O are at or very close to the black line, which means that the bond orders at those correlation points were almost conserved. As shown in Fig. 4, the q_1 values of H_{10} correlation points at the TS are a bit positive, which indicates that H_{10} moves more than halfway from N_1 to O_{11} and is close to O_{11}. The q_1 values of H_{12} correlation points at the TS are very negative, which indicates that H_{12} rarely moves and is still very close to O_{11}. Hence, H_3O^+-like structure appears as part of TS. The correlation plot proves that ESPT process in the 3-*R*-2,7-DAI-H_2O complex occurs concertedly but highly asynchronously.

3.3 ESPT energetics

We calculated the reaction energies (ΔE) and the barrier heights (ΔV) of ESPT in the 3-*R*-2,7-DAI-H_2O (*R*: CH_3, C_2H_5, NH_2, CF_3, CN) complex and listed those data in Table 4. The reaction energies with and without zero-point energy (ZPE) corrections of 3-*R*-2,7-DAI-H_2O are in the range of − 13.3 to − 16.1 kcal/mol and − 3.7 to − 1.5 kcal/mol, respectively. The ESPT processes in the 3-*R*-2,7-DAI-H_2O complex are obviously exothermic. The ESPT barrier heights without and with ZPE-corrected in the 3-*R*-2,7-DAI-H_2O complex are in the range of 8.91–12.0 kcal/mol and 6.49–8.65 kcal/mol, respectively. Evidently, the barrier height of ESPT in the 3-*R*-2,7-DAI-H_2O complex varied with the substituted group.

3.4 Substituent effect

In order to study the roles of different substituent to the ESPT process in the 2,7-DAI-H_2O, we compared the results of ESPT in the 3-*R*-2,7-DAI-H_2O (*R*: CH_3, C_2H_5, NH_2, CF_3, CN) complex with those in 2,7-DAI-H_2O [58]. It is obvious that the nature of tautomerization in the 3-*R*-2,7-DAI-H_2O complex is $\pi \rightarrow \pi^*$ transition no matter which substituent R is introduced. The ESPT processes in the 3-*R*-2,7-DAI-H_2O complex all occur in a highly asynchronous but concerted protolysis pattern. Except those similarities during the proton transfer process, the introducing substituent also causes some differences in the 3-*R*-2,7-DAI-H_2O complex.

At first, the absorption peak and fluorescence peaks of N_1–H and N_7–H forms of 3-*R*-2,7-DAI-H_2O change with substituted group R. When the H atom at C_3 position in the 2,7-DAI-H_2O complex is replaced by the electron-donating group (CH_3, C_2H_5, NH_2), the absorption peaks red-shift about 8–38 nm, and the fluorescence peaks red-shift about 18–252 nm. Hence, Stokes shifts of 3-*R*-2,7-DAI-H_2O (*R*: CH_3, C_2H_5, NH_2) complex is averagely increased 32 nm by introducing the electron-donating groups. On the contrary, the replacement of electron-withdrawing group (CF_3, CN) averagely blue-shifted the absorption and fluorescence peaks of N_1–H form of 2,7-DAI-H_2O complex by 3.5 nm and 8 nm, respectively, which makes the Stokes shifts of 3-CF_3-2,7-DAI-H_2O and 3-CN-2,7-DAI-H_2O decrease by only 4.5 nm on average.

Secondly, the H-bond distances of reactant and product in the 3-*R*-2,7-DAI-H_2O (*R*: CH_3, C_2H_5, NH_2, CF_3, CN) complex are affected by different substituent obviously. Compared to the corresponding structural parameters of 2,7-DAI-H_2O, the introducing electron-donating groups (CH_3, C_2H_5, NH_2) averagely elongate the H_{10}–O_{11} distance in reactant and O_{11}–H_{12} distance in product by 0.024 Å and 0.032 Å, respectively. The H_{12}–N_7 distance in reactant and the N_1–H_{10} distance in product averagely shorten by 0.044 Å and 0.057 Å, respectively, by introducing electron-donating group (CH_3, C_2H_5, NH_2). The changes of the H-bond distances in the reactant and product caused by the electron-withdrawing group (CF_3, CN) are completely opposite to

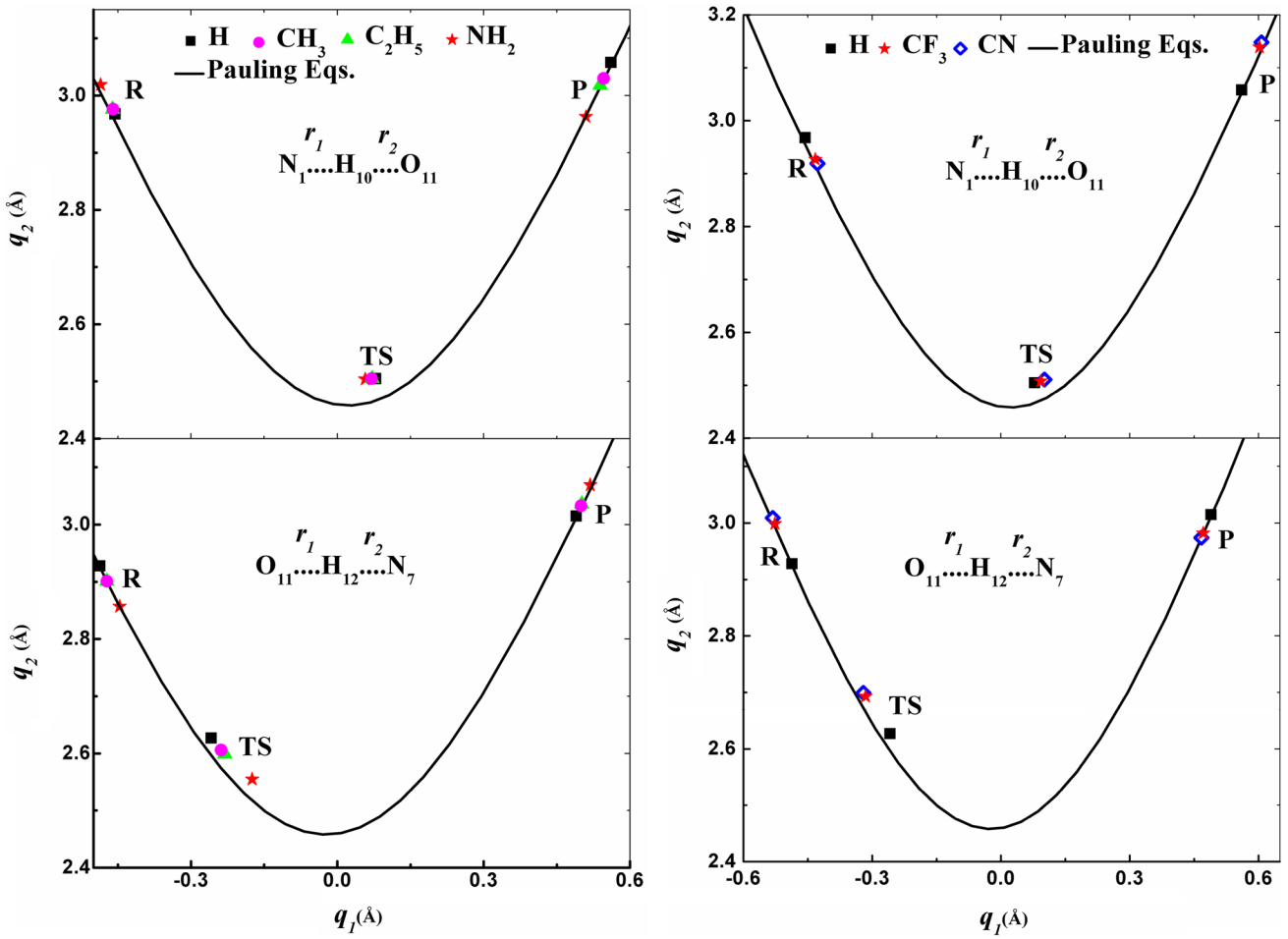

Fig. 4 Correlation of the H-bond distances, $q_2 = r_1 + r_2$, with the proton transfer coordinate, $q_1 = 1/2(r_1 - r_2)$, for **a** 3-*R*-2,7-DAI-H_2O (*R*: H, CH_3, C_2H_5, NH_2), **b** 3-*R*-2,7-DAI-H_2O (*R*: CF_3, CN) complex in water. Top: H_{10} transfer; bottom: H_{12} transfer. All points are for the reactant (*R*), transition state (TS) and product (P) in S_1 optimized at the TD-M06-2X/6–311 + G(d, p) level. The solid lines designate the correlation that satisfies conservation of the bond order. The parameters for Pauling equations were from the literature [83]. The correlation points of 2,7AI-H_2O complex are from the literature [58]. The regions above and below the black line are where the sums of bond orders are smaller and larger than unity, respectively

Table 3 The Hammett (σ_p)[a] substituent constant of substituent groups R (*R*: H, CH_3, C_2H_5, NH_2, CF_3, CN), the distance (Å) between two adjacent heavy atoms in the reactant and TS (in parenthesis), and the Mulliken charge (a.u.) of the H_3O^+-like part of the TS in the 3-*R*-2,7-DAI-H_2O (*R*: H, CH_3, C_2H_5, NH_2, CF_3, CN) complex in S_1 state

System	σ_p	r(N_1–O_{11}) R_1	r(O_{11}–N_7) R_2	$R_1 + R_2$	$\Delta(R_1 + R_2)$[b]	H_3O^+ charge
2,7-DAI-H_2O[c]		2.748(2.405)	2.799(2.519)	5.547(4.924)	0.623	0.791
3-CH_3-2,7-DAI-H_2O	−0.17	2.752(2.403)	2.783(2.503)	5.535(4.906)	0.629	0.802
3-C_2H_5-2,7-DAI-H_2O	−0.15	2.755(2.404)	2.781(2.498)	5.536(4.902)	0.634	0.806
3-NH_2-2,7-DAI-H_2O	−0.66	2.782(2.399)	2.762(2.464)	5.544(4.863)	0.681	0.752
3-CF_3-2,7-DAI-H_2O	0.54	2.724(2.412)	2.833(2.564)	5.557(4.976)	0.581	0.858
3-CN-2,7-DAI-H_2O	0.66	2.721(2.416)	2.836(2.569)	5.557(4.985)	0.572	0.859

[a]Data from Ref. [75]

[b]$\Delta(R_1 + R_2)$ is the difference between the sum of the R_1 and R_2 distances in the reactant and those values at the TS

[c]Data from Ref. [58]

Table 4 Reaction energies (ΔE) and barrier heights (ΔV) for excited-state proton transfer in the 3-*R*-2,7-DAI-H_2O (*R*: H, CH_3, C_2H_5, NH_2, CF_3, CN) complex in the S_1 state

System	ΔE (kcal/mol)	ΔV (kcal/mol)
2,7-DAI-H_2O[a]	− 16.2(− 15.5)	9.98(7.24)
3-CH_3-2,7-DAI-H_2O	− 16.1(− 15.7)	10.2(7.28)
3-C_2H_5-2,7-DAI-H_2O	− 15.5(− 15.1)	10.5(7.61)
3-NH_2-2,7-DAI-H_2O	− 13.7(− 13.3)	12.0(8.64)
3-CF_3-2,7-DAI-H_2O	− 16.5(− 16.1)	8.91(6.49)
3-CN-2,7-DAI-H_2O	− 16.1(− 15.4)	8.95(6.90)

The numbers in parentheses include zero-point energies

[a]Data from Ref [58]

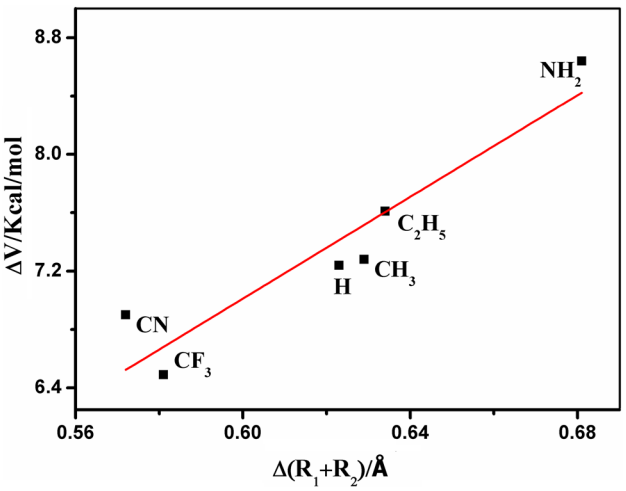

Fig. 5 Correlation of the difference $\Delta(R_1+R_2)$ between the sum of the N_1-O_{11} (R_1) and $O_{11}-N_7$ (R_2) distances in the reactant and those values in the TS with the ZPE-corrected barrier height (ΔV) of ESPT in 3-*R*-2,7-DAI-H_2O (*R*: H, CH_3, C_2H_5, NH_2, CF_3, CN) complex

those caused by the electron-donating group (CH_3, C_2H_5, NH_2). As a result, the distance between two adjacent end atoms (such as N_1-O_{11} and $O_{11}-N_2$) varied with the substituent. H-bond compression can reduce the barrier [83]. Namely, the distances of N_1-O_{11} (R_1) and $O_{11}-N_7$ (R_2) can influence the ESPT barrier height. As shown in Table 3, the sum of R_1 and R_2 in the 3-*R*-2,7-DAI-H_2O complex are in the range of 5.535–5.557 Å in the reactant and in the range of 4.863 ~ 4.985 Å in the TS, respectively. We used $\Delta(R_1+R_2)$ to represent the difference between (R_1+R_2) in the reactant and that in the TS. For the 3-*R*-2,7-DAI-H_2O (*R*: CH_3, C_2H_5, NH_2) complex, $\Delta(R_1+R_2)$ is on average 0.025 Å longer than the corresponding distance of 2,7-DAI-H_2O, which indicates that ESPT process in the 3-*R*-2,7-DAI-H_2O (*R*: CH_3, C_2H_5, NH_2) complex is much harder than that in the 2,7-DAI-H_2O. When the electron-withdrawing group (CF_3, CN) is introduced in the 2,7-DAI-H_2O, ESPT process would be much easier due to the shorter $\Delta(R_1+R_2)$ value. The ESPT barrier height and $\Delta(R_1+R_2)$ in the 3-*R*-2,7-DAI-H_2O (*R*: CH_3, C_2H_5, NH_2, CF_3, CN) complex have a good correlation (see Fig. 5). The $\Delta(R_1+R_2)$ value and Mulliken charge of H_3O^+ in the 3-*R*-2,7-DAI-H_2O (*R*: CH_3, C_2H_5, NH_2, CF_3, CN) complex also have linear dependence on the Hammett's constant of R (see Fig. 6).

Thirdly, the geometrical parameters in the TS of 3-*R*-2,7-DAI-H_2O (*R*: CH_3, C_2H_5, NH_2, CF_3, CN) changed with the substituted group. For 3-*R*-2,7-DAI-H_2O (*R*: CH_3, C_2H_5, NH_2), the N_1-H_{10} and $H_{12}-N_7$ distances are on average 0.012 Å and 0.064 Å shorter than the corresponding values in the 2,7-DAI-H_2O complex, and the $H_{10}-O_{11}$ and $O_{11}-H_{12}$ distances are on average 0.012 Å and 0.024 Å longer than those values in the 2,7-DAI-H_2O complex. The influence to the geometrical parameters from the introducing electron-withdrawing group (CF_3, CN) is totally contrary with comparison to introducing electron-donating group (CH_3, C_2H_5, NH_2). Such changes on the structures result in a few differences in the correlation plot. As shown in Fig. 4a, H10 and H12 correlation points for TS in the 3-*R*-2,7-DAI-H_2O (*R*: CH_3, C_2H_5, NH_2) complex move slightly to the left side and a little to the right side, respectively, along the Pauling curve with comparison to the corresponding points in the 2,7-DAI-H_2O complex. Hence, positions of H_{10} and H_{12} transfer reaction coordinate in the 3-*R*-2,7-DAI-H_2O (*R*: CH_3, C_2H_5, NH_2) complex are slightly late and a little early, respectively, which means that the asynchronicity of ESPT was reduced by introduction of the electron-donating group (CH_3, C_2H_5, NH_2). For 3-*R*-2,7-DAI-H_2O (*R*: CF_3, CN) complex, H_{10} and H_{12} correlation points for TS shift a trifle to right and a little to left along the Pauling curve, which leads to the positions of H_{10} and H_{12} transfer reaction coordinate are a trifle early and a little late, respectively. The introduction of electron-withdrawing group (CF_3, CN) enlarges the asynchronicity of ESPT (see Fig. 4b).

Lastly, the barrier heights of ESPT process in the 3-*R*-2,7-DAI-H_2O (*R*: CH_3, C_2H_5, NH_2, CF_3, CN) complex are obviously influenced by the substituent. The electron-donating group (CH_3, C_2H_5, NH_2) averagely increases the barrier height by 0.60 kcal/mol, and the electron-withdrawing group (CF_3, CN) averagely reduces the barrier height by 0.36 kcal/mol.

4 Conclusions

In this work, we investigated the substituent effect on the ESPT process in the 3-*R*-2,7-DAI-H_2O (*R*: CH_3, C_2H_5, NH_2, CF_3, CN) complex in detail at the TD-M06-2X/6–311 + G(d, p) level. Our theoretical results showed that ESPT in the title complex preferred to occur in a concerted but highly asynchronous protolysis pattern regardless of electron-donating

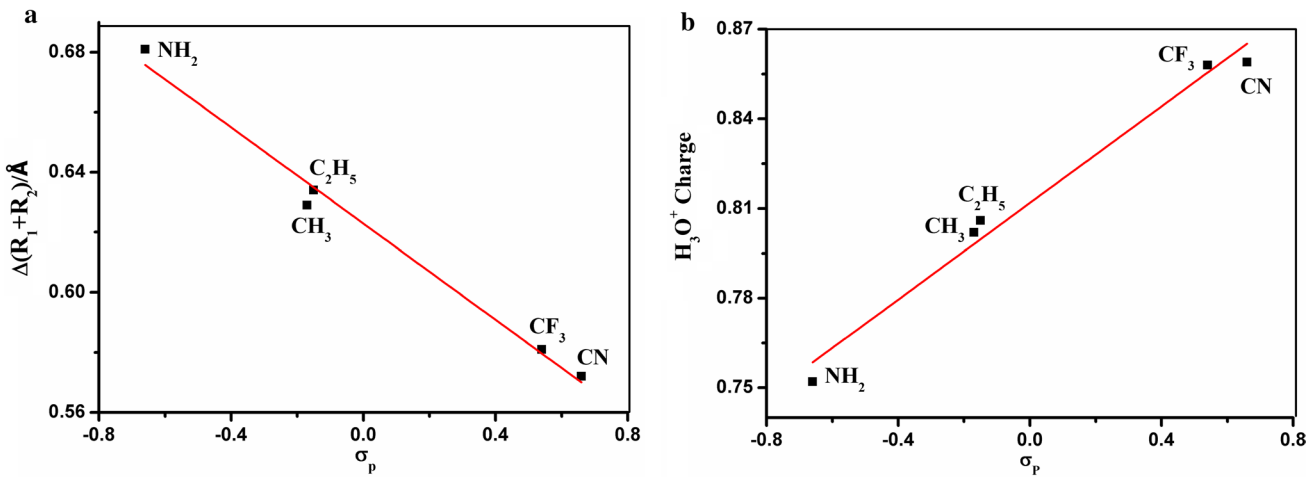

Fig. 6 Correlation between Hammett's substituent constant and **a** the difference $\Delta(R_1+R_2)$ between the sum of the N_1-O_{11} (R_1) and $O_{11}-N_7$ (R_2) distances in the reactant and those values in the TS, **b** Mulliken charge of H_3O^+-part in the TS in 3-*R*-2,7-DAI-H_2O (*R*: CH_3, C_2H_5, NH_2, CF_3, CN) complex

or electron-withdrawing group. Along this pathway, proton H_{10} triggered the ESPT process and shifted more than halfway from N_1 to O_{11}, proton H_{12} transferred little from O_{11} to N_7 simultaneously, then a H_3O^+-like moiety was formed at O_{11}. Different substituent at C_3 position in the 2,7-DAI-H_2O complex had an evident effect on the H-bond distances and lead to the N_1-O_{11} (R_1) and $O_{11}-N_7$ (R_2) distances varied with the substituent. The $\Delta(R_1+R_2)$ value and the ESPT barrier height had a good correlation. The $\Delta(R_1+R_2)$ value and Mulliken charge of H_3O^+ also have linear dependence on the Hammett's substituent constant. The replacement of different substituent affected the structural parameters of TS. Hence, the asynchronicity of proton transfer was enlarged or reduced by the electron-withdrawing group (CF_3, CN) or electron-donating group (CH_3, C_2H_5, NH_2), respectively. The barrier height of ESPT process averagely decreased or increased 0.36 and 0.60 kcal/mol by the electron-withdrawing group or the electron-donating group. The electron-donating group red-shifted the absorption and fluorescence emission peaks with different increments on absorption and fluorescence bands, respectively, which resulted in increasing the Stokes shift obviously. Whereas the electron-withdrawing group blue-shifted the absorption and fluorescence emission peaks with similar decrement on absorption and fluorescence bands, which led to a slight decrease in the Stokes shift.

References

1. Dybala-Defratyka A, Paneth P, Pu J, Truhlar D (2004) J Phys Chem A 108:2475
2. Han K, He G (2007) J Photochem Photobiol C: Photochem Rev 8:55
3. Pietrzak M, Shibl M, Broring M, Kuhn O, Limbach H (2007) J Am Chem Soc 129:296
4. Olsen S, Smith SC (2008) J Am Chem Soc 130:8677
5. Raymo FM, Bartberger MD, Houk KN, Stoddart JF (2001) J Am Chem Soc 123:9264
6. Cramer CJ, Truhlar DG (2008) Acc Chem Res 41:760
7. Zhao G, Han K (2007) J Phys Chem A 111:2469
8. Zhao G, Liu J, Zhou L, Han K (2007) J Phys Chem B 111:8940
9. Zhao G, Northrop B, Stang P, Han K (2010) J Phys Chem 114:3418
10. Zhao G, Han K (2010) Phys Chem Chem Phys 12:8914
11. Zhao G, Han K (2012) Acc Chem Res 45:404
12. Kungwan N, Kerdpol K, Daengngern R, Hannongbua S (2014) Barbatti M 133:1480
13. Savarese M, Brémond É, Adamo C, Rega N, Ciofini I (2016) Chem Phys Chem 17:1530
14. Wilbraham L, Savarese M, Rega N, Adamo C, Ciofini I (2015) J Phys Chem B 119:2459
15. Rini M, Magnes BZ, Pines E, Nibbering ETJ (2003) Science 301:349
16. Siwick BJ, Bakker HJ (2007) J Am Chem Soc 129:13412
17. Savarese M, Netti PA, Adamo C, Rega N, Ciofini I (2013) J Phys Chem B 117:16165
18. Wang Y, Liu W, Tang L, Oscar B, Han F, Fang C (2013) J Phys Chem A 117:6024
19. Raucci U, Savarese M, Adamo C, Ciofini I, Rega N (2015) J Phys Chem B 119:2650
20. Petrone A, Cimino P, Donati G, Hratchian HP, Frisch MJ, Rega N (2016) J Chem Theory Comput 12:4925
21. Zhou PW, Han KL (2018) Acc Chem Res 51:1681
22. Chiariello MG, Rega N (2018) J Phys Chem A 122:2884
23. Donati G, Petrone A, Caruso P, Rega Nadia (2018) Chem Sci 9: 1126
24. Amoruso G, Taylor VCA, Duchi M, Goodband E, Oliver TAA (2019) J Phys Chem B 123:4745
25. Negreie M, Bellefeuille SM, Whitham S, Petrich JW, Thornburg RW (1990) J Am Chem Soc 112:7419

26. Smirnov AS, English DS, Rich RL, Lane J, Teyton L, Schwabacher AW, Luo S, Thornburg RW, Petrich JW (1997) J Phys Chem B 101:2758
27. Negrerie M, Gai F, Bellefeuille SM, Petrich JW (1991) J Phys Chem 95:8663
28. Douhal A, Kim SK, Zewail AH (1995) Nature 378:260
29. Chachisvilis M, Fiebig T, Douhal A, Zewail AH (1998) J Phys Chem A 102:669
30. Fiebig T, Chachisvilis M, Manger M, Zewail AH, Douhal A, Garcia-Ochoa I, de La Hoz AA (1999) J Phys Chem A 103:7419
31. Moreno M, Douhal A, Lluch JM (2001) J Phys Chem A 105:3887
32. Guallar V, Batista VS, Miller WH (1999) J Chem Phys 110:9922
33. Kwon OH, Zewail AH (2007) Proc Natl Acad Sci USA 104:8703
34. Takeuchi S, Tahara T (1998) J Phys Chem A 102:7740
35. Catalán J, Prez P, del Valle JC, de Paz JLG, Kasha M (2002) Proc Natl Acad Sci USA 99:5799
36. Catalán J, Prez P, del Valle JC, de Paz JLG, Kasha M (2004) Proc Natl Acad Sci USA 101:419
37. Sakota K, Hara A, Sekiya H (2004) Phys Chem Chem Phys 6:32
38. Sakota K, Sekiya H (2005) J Phys Chem A 109:2718
39. Sakota K, Sekiya H (2005) J Phys Chem A 109:2722
40. Sakota K, Okabe C, Nishi N, Sekiya H (2005) J Phys Chem A 109:5245
41. Catalän J, de Paz JLG (2005) J Chem Phys 123:114302
42. Takeuchi S, Tahara T (2007) Proc Natl Acad Sci USA 104:5285
43. Folmer DE, Wisniewski ES, Stairs JR, Castleman AW Jr (2000) J Phys Chem A 104:10545
44. Schowen RL (1997) Angew Chem Int Ed 36:1434
45. Kwon OH, Lee YS, Park HJ, Kim Y, Jang DJ (2004) Angew Chem Int Ed 43:5792
46. Avouris P, Yang LL, El-Bayoumi MA (1976) Photochem Photobiol 24:211
47. Collins ST (1983) J Phys Chem 87:3202
48. Chou PT, Martinez ML, Cooper WC, McMorrow D, Collin ST, Kasha M (1992) J Phys Chem 96:5203
49. Chapman CF, Maroncelli M (1992) J Phys Chem 96:8430
50. Chen Y, Rich RL, Gai F, Petrich JW (1993) J Phys Chem 97:1770
51. Ross JB, Szabo AG, Hogue CW (1997) Methods Enzymol 278:151
52. Rich RL, Smirnov AV, Schwabacher AW, Petrich JW (1995) J Am Chem Soc 117:11850
53. Hoesl MG, Larregola M, Cui H, Budisa N (2010) J Pept Sci 16:589
54. Chen Y, Gai F, Petrich JW (1994) J Phys Chem 98:2203
55. Shen JY, Chao WC, Liu C, Pan HA, Yang HC, Chen CL, Lan YK, Lin LJ, Wang JS, Lu JF, Chou SCW, Tang KC, Chou PT (2013) Nat Commun 4:2611
56. Chou PT, Chi Y (2007) Chem Eur J 13:380
57. Liu Y, Tang Z, Wang Y, Tian J, Fei X, Cao F, Li GU (2017) Spec Acta A Mol Biomol Spec 187:163
58. Fang H (2019) Spec Acta A Mol Biomol Spec 214:152
59. Chen KY, Hsieh CC, Cheng YM, Lai CH, Chou PT (2006) Chem Commun 13:4395
60. Hsieh CC, Cheng YM, Hsu CJ, Chen KY, Chou PT (2008) J Phys Chem A 112:8323
61. Hristova S, Dobrikov G, Kamounah FS, Kawauchi S, Hansen PE, Deneva V, Nedeltcheva D, Antonov L (2015) RSC Adv 5:102495
62. Li CZ, Yang YG, Ma C, Liu YF (2016) RSC Adv 6:5134
63. Marciniak H, Hristova S, Deneva V, Kamounah FS, Hansen PE, Lochbrunner S, Antonov L (2017) Phys Chem Chem Phys 19:26621
64. Yi JC, Fang H (2018) Struct Chem 29:1341
65. Frisch MJ, Truck GW, Schlegel HB, Scuseria GE, Robb MA, Cheeseman JR, Scalmani G, Barone V, Mennucci B, Petersson GA, Nakatsuji H, Caricato M, Li X, Hratchian HP, Izmaylov AF, Bloino J, Zheng G, Sonnenberg JL, Hada M, Ehara M, Toyota K, Fukuda R, Hasegawa J, Ishida M, Nakajima T, Honda Y, Kitao O, Nakai H, Vreven T, Montgomery JA Jr, Peralta JE, Ogliaro F, Bearpark M, Heyd JJ, Brothers E, Kudin KN, Staroverov VN, Kobayashi R, Normand J, Raghavachari K, Rendell A, Burant JC, Iyengar SS, Tomasi J, Cossi M, Rega N, Millam JM, Klene M, Knox JE, Cross JB, Bakken V, Adamo C, Jaramillo J, Gomperts R, Stratmann RE, Yazyev O, Austin AJ, Cammi R, Pomelli C, Ochterski JW, Martin RL, Morokuma K, Zakrzewski VG, Voth GA, Salvador P, Dannenberg JJ, Dapprich S, Daniels AD, Farkas O, Foresman JB, Ortiz JV, Cioslowski J, Fox DJ (2009) Gaussian 09, Rev. D01, Gaussian, Inc, Wallingford CT.
66. Zhao Y, Truhlar DG (2008) Theor Chem Acc 120:215
67. Cancès E, Mennucci B, Tomasi J (1997) J Chem Phys 107:3032
68. Cossi M, Barone V, Mennucci B (1998) Chem Phys Lett 286:253
69. Mennucci B, Tomasi J (1997) J Chem Phys 106:5151
70. Tanner C, Manca C, Leutwyler S (2003) Science 302:1736
71. Fang WH (1999) J Am Chem Soc 103:5567
72. Tanner C, Manca C, Leutwyler S (2005) J Chem Phys 122:204326
73. Ashfold MNR, Cronin B, Devine AL, Dixon RN, Nix MGD (2006) Science 312:1637
74. Mohammed OF, Pines D, Nibbering ETJ, Pines E (2007) Angew Chem Int Ed 46:1458
75. Hansch C, Leo A, Taft RW (1991) Chem Rev 91:165
76. Limbach HH, Pietrzak M, Benedict H, Tolstoy PM, Golubev NS, Denisov GS (2004) J Mol Struct 706:115
77. Limbach HH, Lopez JM, Kohen A (2006) Philos Trans R Soc B 361:1399
78. Limbach HH (2007) In hydrogen-transfer reactions. Schowen RL, Klinman JP, Hynes JT, Limbach HH (eds). Wiley, Weinheim, Chapter 6, pp 135–221.
79. Brown ID (1992) Acta Cryst B 48:553
80. Dos A, Schimming V, Tosoni S, Limbach HH (2008) J Phys Chem B 112:15604
81. Garrett BC, Truhlar DG (1979) J Am Chem Soc 101:4534
82. Johnston HS (1966) Gas phase reaction rate theory. Ronald Press, New York, pp 1–362
83. Limbach HH, Schowen KB, Schowen RL (2010) J Phys Org Chem 23:586